Building Technologies & Urban Systems Division
Energy Technologies Area
Lawrence Berkeley National Laboratory

Comparison of Airflow and Acoustic Measurements for Evaluation of Building Air Leakage Paths in a Laboratory Test Apparatus

Benedikt Kölsch[1]
Iain Walker[2]
Woody Delp[2]
Björn Schiricke[1]
Bernhard Hoffschmidt[1]

1 – Instiute of Solar Research, German Aerospace Center (DLR)
2 - Lawrence Berkeley National Laboratory

Energy Technologies Area
May 2022

Disclaimer

This document was prepared as an account of work sponsored by the United States Government. While this document is believed to contain correct information, neither the United States Government nor any agency thereof, nor the Regents of the University of California, nor any of their employees, makes any warranty, express or implied, or assumes any legal responsibility for the accuracy, completeness, or usefulness of any information, apparatus, product, or process disclosed, or represents that its use would not infringe privately owned rights. Reference herein to any specific commercial product, process, or service by its trade name, trademark, manufacturer, or otherwise, does not necessarily constitute or imply its endorsement, recommendation, or favoring by the United States Government or any agency thereof, or the Regents of the University of California. The views and opinions of authors expressed herein do not necessarily state or reflect those of the United States Government or any agency thereof or the Regents of the University of California.

This work was supported by the Assistant Secretary for Energy Efficiency and Renewable Energy, Building Technologies Office, of the U.S. Department of Energy under Contract No. DE-AC02-05CH11231 and the German Aerospace Center (DLR), which is funded by the German Ministry for Economic Affairs and Energy [grant number 03ET1405A].

Also published as:
Kölsch, B, Walker, I., Delp, W., Schricke, B. and Hoffschmidt, B. (2022). Comparison of Airflow and Acoustic Measurements for Evaluation of Building Air Leakage Paths in a Laboratory Test Apparatus. Proc. IAQ 2020. Proc. AIVC/ASHRAE IAQ 2020 Conference, Athens, Greece.

ABSTRACT

Unintended Infiltration in buildings is responsible for a significant portion of the global housing stock energy demand. Today, the fan pressurization method, also known as blower-door test, is the most frequently used measurement method to evaluate the airtightness of buildings and determining the total air change rate of a building or a building element. However, the localization and quantification of single leaks in the building envelope remain difficult and time-consuming. In this paper, an acoustic method is introduced to estimate the leakage size of single leaks in buildings. Sound transmission measurements and measurements of airflow have been conducted in a laboratory test apparatus. The objective of this investigation is to compare acoustic measurements with airflow measurements of leaks under the same boundary conditions. The test apparatus consists of two chambers, which are separated by a test wall. This test wall represents a single characteristic air leakage path in the building envelope. Various types of wall structures with different slit geometries, wall thicknesses and insulation materials have been investigated. The acoustic measurements have been performed with a sound source placed in one chamber and ultrasonic microphones located in both chambers. The results of the acoustic measurements were compared to airflows through the test wall measured using a flow nozzle to provide estimates of the uncertainty in the acoustic approach.

INTRODUCTION

Buildings are responsible for almost a third of the global final energy consumption and account for an equally large share of global CO2 emissions (International Energy Agency 2011). The airflow through building envelope has a significant contribution to an increase of heating and cooling energy in residential buildings. Therefore, the knowledge of unintended infiltration in buildings is essential. The most frequently used technique to assess the airtightness of buildings and compare them among each other is the fan pressurization method (also known as "blower-door test"). This method is described in various standards like ASTM E779 (ASTM 2019), DIN EN ISO 9972 (DIN 2018) or CAN/CGSB 149.10 (CAN/CGSB 2019). The fan pressurization method serves the purpose of measuring airtightness to meet requirements to fulfill specific energy performance standards, comparing relative airtightness of different buildings among each other or determining the reduction of air permeability after refurbishments. In order to reduce air leakage in existing buildings it is necessary to identify leak locations and prioritize sealing of larger leaks. In addition, knowledge of leak location can be used to improve estimates of infiltration airflows (Walker and Wilson 1998). However, quantification and identification of single leaks are challenging and time-consuming. The use of supplementary acoustic methods has the potential to support current air leakage measurement methods.

One possible approach has already been suggested in the ASTM E1186 (ASTM 2017) standard. Among other methods like building pressurization and tracer gas detection, this standard recommends the use of sound detection, which is rarely applied in buildings. Locating leaks by sound detection has been investigated in laboratory environments (Muehleisen, R. and Chelliah 2018; Chelliah et al. 2017) and single-frequency transmission attenuation has been examined in both laboratory and field testing with some success (Varshney et al. 2013).

This study attempts to determine the magnitude of leakage airflow using a multi-frequency approach. In addition to the method prescribed in the ASTM standard, this paper will focus more on the quantification of airflow through single leaks than on the detection of leaks in the building envelope using sound. In this work, the evaluation of single leak structures and a comparison between the fan pressurization method and an acoustic approach in a laboratory test apparatus has been performed.

EXPERIMENTAL SETUP

A wooden test box was chosen as an experimental setup and is shown in Figure 1. The box has a total length of 2.5 m and a height and depth of 0.6 m. It consists of two chambers with a length of one chamber of 1.1 m. Both chambers are separated from each other with test walls, where different leaks are investigated. The box is made of medium-density fiberboard (MDF). For all measurements, the box is closed and air sealed with a lid on top.

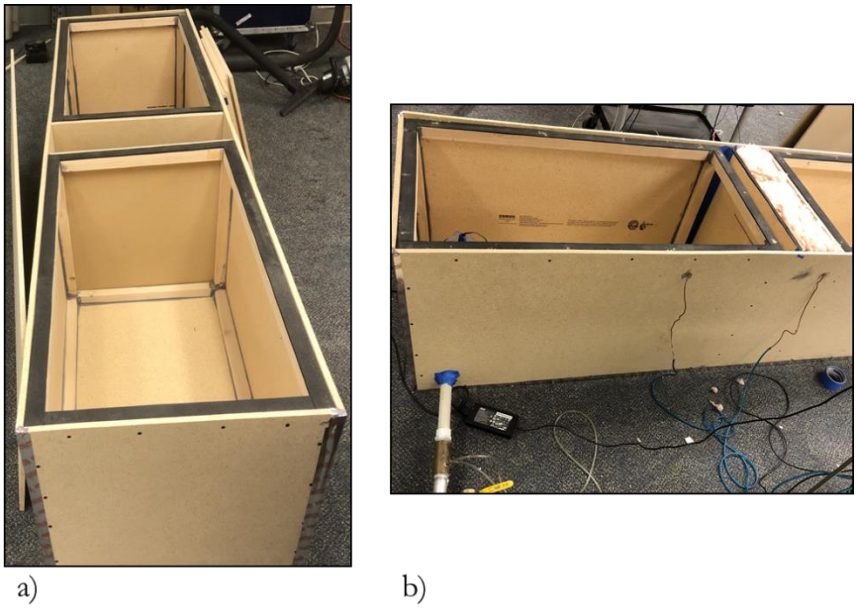

Figure 1: Test box top view (a) and side view with blower and pressure taps (b)

Investigated Wall Structures

In this paper, 26 different wall structures have been studied in order to simulate realistic leakage scenarios for individual leaks. The following wall parameters have been modified between measurements:

- The number of walls: a single wooden wall with a slit in the upper part of the wall or two walls with slits and an air gap between them (see Figure 2 (a) and (b)). The slit has a length of 180 mm.
- Different distances between the double-wall constructions: 100 and 150 mm (see Figure 2 (b) and (c)). These distances are in the magnitude of typical wall thicknesses.
- Measurements with and without insulating material (glass wool) in between two walls (see Figure 2 (d)).
- Connection of the slits at a double wall with a canal (see Figure 2 (e)).
- Variation of the slit height: 5, 1, 0.4, 0.25 mm (see Figure 2 (f)).
- A blank wall panel with no openings.

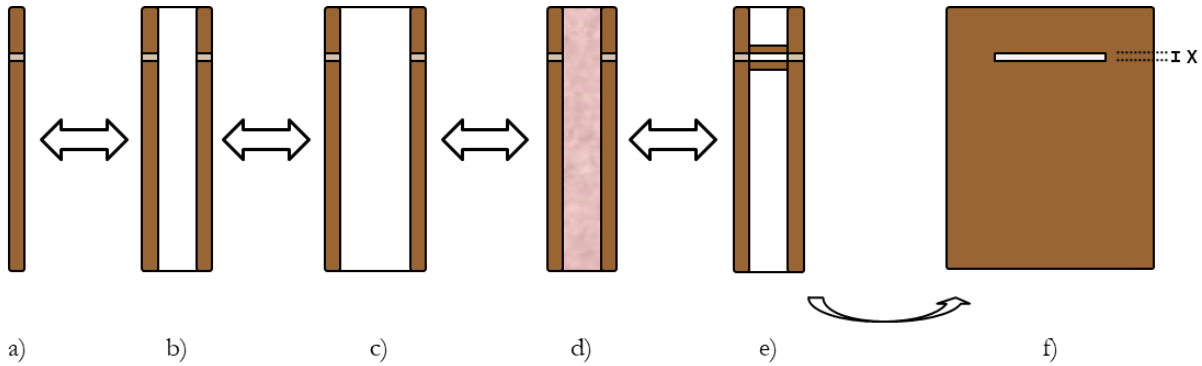

Figure 2: Illustrations of investigated wall structures with slits: single wall (a), double wall (b), increasing air gaps (c), additional insulation material (d), connected slits (e) and varying slit heights (f)

Airflow and Pressure difference Measurements

Similar to the ASTM E779 (ASTM 2019) standard, which describes the application of the fan pressurization method in a whole building or single rooms, a blower was installed in the previously described test apparatus. The blower was connected to one of the two chambers and is shown in Figure 3 (a). This pressurized chamber was sealed and the second chamber was open to ambient conditions. The airflow of this blower was controlled with a manual valve and a blower speed controller. In this experiment, only pressurized and no depressurized tests have been performed. The results of depressurization measurements are expected to be the same because the leak configurations remain rigid and symmetrical during the tests and therefore, will not change between pressurized and depressurized tests.

The airflow was measured with a Venturi airflow meter installed between blower and box and is shown in Figure 3 (b). A Venturi airflow meter consists of a cylinder at the entrance, a convergent section, a throat and a divergent section, as illustrated in Figure 3 (c). The contraction of the pipe diameter results, according to Bernoulli's principle, in an increase of fluid velocity and a decrease of the static pressure along a streamline. From the measurement of this static pressure difference (ΔP), the airflow (Q) through the tube can be calculated using Bernoulli's principle and continuity equation (Reader-Harris 2015).

This correlation is described in Equation (1), where A_1 and A_1 are the cross-sectional areas at the positions where the pressure measurements were taken, and ρ is the density of air. The positions of the pressure measurement taps [1] and [2] are shown in Figure 3 (b) and (c).

$$\mathrm{Q} = A_1 \sqrt{\frac{2}{\rho\left(\left(\frac{A_1}{A_2}\right)^2 - 1\right)}} \cdot \sqrt{\Delta P_{1-2}} \qquad (1)$$

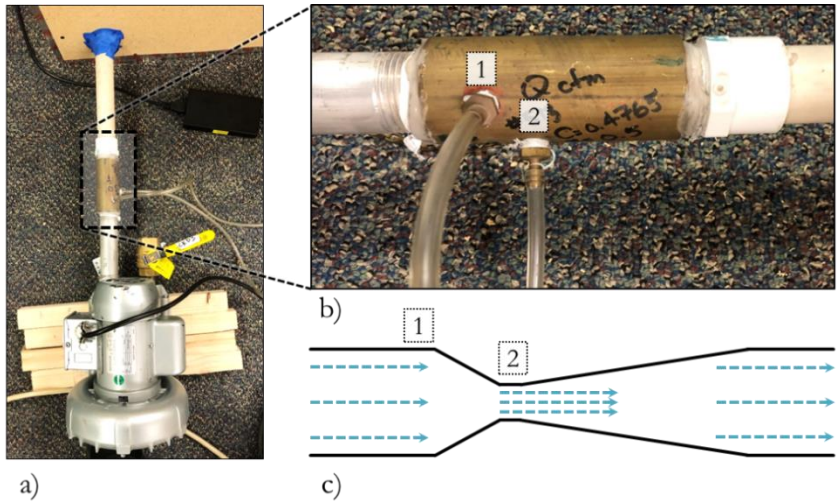

Figure 3: Blower with manual valve (a), Venturi airflow meter with pressure taps (b) and a schematic illustration of the Venturi airflow meter (c)

The pressure in the pressurized chamber was measured with a copper tube near the inner wall in that chamber. Due to the open second chamber to ambient conditions, the pressure difference between both chambers can easily be determined. A second pressure measurement was installed inside the double-wall structures (Figure 1(b) and (c)) to monitor the pressure difference inside the wall structure as well. With the measurement of pressure difference across the test walls and the airflow through the walls, the pressure exponent n and flow coefficient C of the power law formulation can be obtained for each leak configuration. Equation (2) shows the correlation between airflow and pressure difference using the power law.

$$\mathrm{Q} = C \cdot \Delta P^{n} \tag{2}$$

Acoustic Measurements

Acoustic measurements were performed with a speaker placed together with one microphone in one chamber and another microphone in the other chamber. For these measurements, both chambers were sealed to the ambient conditions. The speaker is an omnidirectional ultrasonic dynamic speaker with a frequency range of 1-120 kHz, and the acoustic transducers are 0.25-inch condenser microphones with an even frequency response and a recommended frequency range of 0.004-100 kHz. The signal which was sent by the speaker consists of discrete sine tones from 0.5 kHz to 80 kHz in ascending 0.5 kHz steps. This signal enables an analysis of a broad frequency range. Although, the spectral resolution is lower compared to a sinus sweep, this signal enables a higher signal-to-noise ratio, because all energy is concentrated at a single frequency for each measurement. According to the Nyquist-Shannon sampling theorem (Shannon 1949), the sampling frequency of the analog-digital converter should be higher than twice the maximum analyzed signal frequency. Thus, the data acquisition has been performed with a USB wide dynamic range signal analyzer with a sampling frequency of 216 kHz per channel and a resolution of 24 bits. An interface between the data logger and measurement computer, as well as the signal generation, was implemented in Python.

The relationship between the signal which is emitted in one chamber and the signal received in the other chamber can be described using the frequency-dependent coherence function. The coherence function is a measure of the linear dependency between two discrete time signals x[n] and y[n]. It describes the fraction of an output signal from an input signal at a specific frequency. This can be characterized by the following equation:

$$C_{xy}(f) = \frac{|G_{xy}(f)|^2}{G_{xx}(f) \cdot G_{yy}(f)} \quad (3)$$

The coherence is calculated by dividing the squared magnitude of the cross-spectral density G_{xy} between x and y with the product of the auto-spectral density of signals x (G_{xx}) and y (G_{yy}). This function is always between 1 and 0, with a value at 0 indicating total independency between both signals at a specific frequency (Benesty and Huang 2013).

RESULTS AND DISCUSSION

Airflow-Pressure Difference Measurements

The airflow and pressure difference measurements have been performed for all leak configurations. Figure 4 shows these measurements as an example of four selected leak configurations. Here, a double-wall construction with a 100 mm distance between both walls, no insulation between these walls and a connecting canal between both parallel slits is shown (cf. Figure 2 (e)). The solid lines show the power law fit (see Equation (2)) to the measurement data (dots). The airflow through the largest slit with a cross-sectional area of 9 cm² (blue) is, as might be expected, the largest. Much smaller is the airflow through slits with a cross-sectional area of 0.7 (green) and 0.4 cm² (magenta).

The three black vertical dotted lines indicate the predicted airflows through these leaks at 50, 10 and 4 Pa pressure difference. 50 Pa pressure difference is a frequently used value for the comparison of blower door measurements of real buildings (DIN 2018), whereas a 10 Pa pressure difference is used in the Canadian CGSB standard (CAN/CGSB 2019) to calculate for instance the equivalent leakage area. At 4 Pa pressure difference or less, natural infiltration usually occurs in buildings, which is an essential metric in indoor air quality applications (Vornanen-Winqvist et al. 2018) and building energy simulations (Ng et al. 2013). This is also the reference pressure most often used when converting to Equivalent Leakage Area (e.g., in the ASTM test method). These pressure levels are chosen as a basis for subsequent comparisons with the acoustic data.

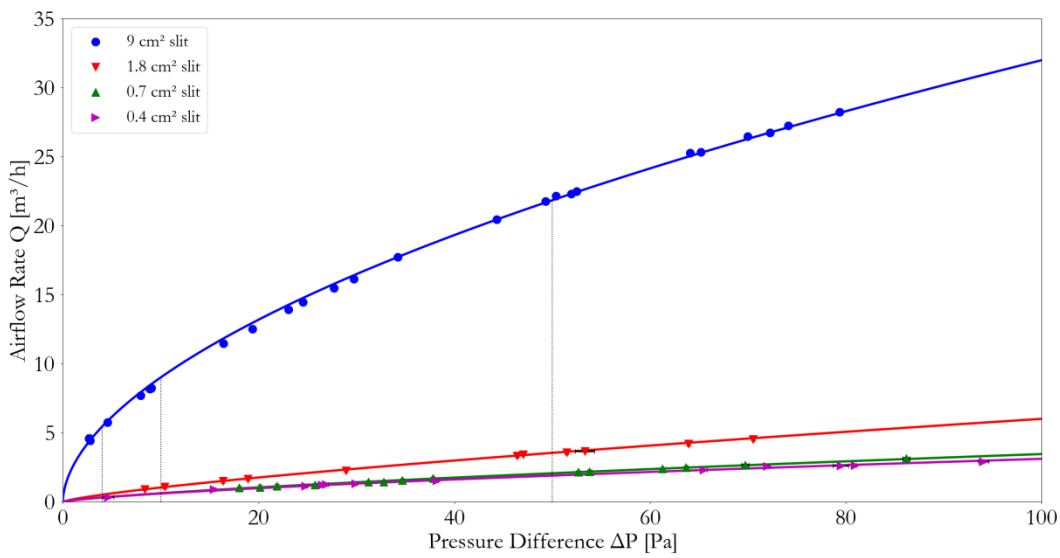

Figure 4: Display of airflow-pressure measurement and power law fit for a double-wall construction with a 100 mm distance between the walls, no insulation and a connection between the slits for four different slit sizes

Acoustic Measurements

The previously described coherence function has been calculated for all investigated leak configurations. To illustrate how coherence changes with frequency we chose a single exmple wall configuration for simplicity. Figure 5 shows measured coherence for a double-wall construction with a 100 mm distance between the walls, no insulation and a connection between the slits for four different slit sizes and a tight double-wall (same as Figure 4). The dotted lines in Figure 5 indicate the mean value of the coherence function over the whole considered frequency spectrum of a given leak. This value increases with an increasing slit size. While there are some changes with frequency, there are no clear trends and the differet test configuraitons have different results. This indicates that it would be reasonable to use a single coherence value averaged over the full frequency range. We therefore used the mean coherence values when assessing the test results for all configurations.

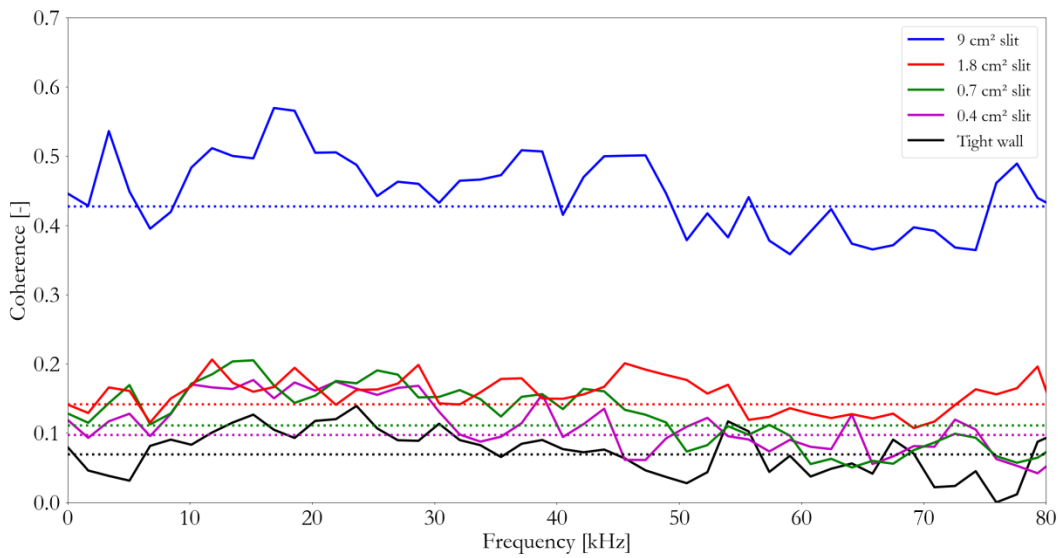

Figure 5: Coherence function for a double-wall construction with a 100 mm distance between the walls, no insulation and a connection between the slits for four different slit sizes and a tight double-wall

As illustrated in Figure 5, there was some sound transmission even with no leaks and the wall panels sealed (the "yight Wall" configuration). To reduce the impact of this sound that is transmitted through the wall structure and to focus more on the sound transmitted via the leaks, we subtracted the mean coherence value of a tight wall from the mean value of the same wall with a specific slit. We performed this subtraction for all test configurations shown in Figure 2 to obtain the results shown in Figure 6, whre the differences between the mean coherence functions and the respective airflow rates at 50 (red), 10 (black) and 4 Pa (green) are displayed.

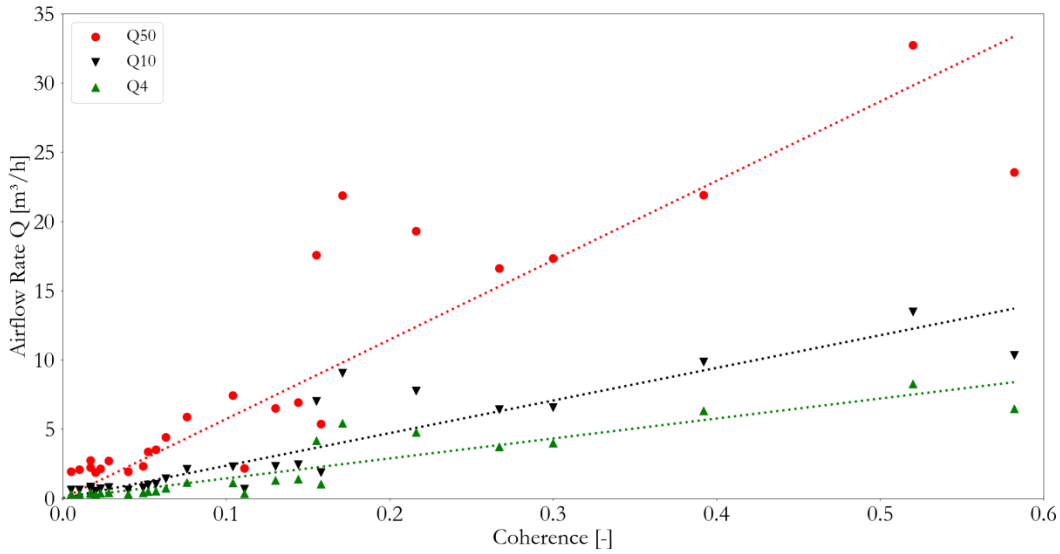

Figure 6: Correlation between mean coherence and different airflow rates for all the investigated leakage configurations in Figure 2

The dotted lines in Figure 6 show the mean trend between coherence and airflow rate. Even though the individual measurements do not always lie exactly on this trend line, there is a clear correlation between leakage and coherence which is encouraging as we further devel op ths technique as a method for estimating air leakage. The coefficient of determination R^2, which determines the goodness-of-fit, is 0.79 for Q_{50}, 0.82 for Q_{10} and 0.83for Q_4. Therefore, the correlation appears to be stronger for the lowest airflow rate at 4 Pa, which may result from a smaller scaling of the pressure values. This correlation may not serve the purpose to exactly predict the airflow, but it may give an order of magnitude.

CONCLUSIONS AND FUTURE WORK

In this work, an acoustic method was proposed for quantifying the air leakage in a laboratory test apparatus. This method was compared with pressurization measurements under the same boundary conditions. Within this laboratory test setup, the acoustic approach was able to give an estimate of the magnitude of airflow, which passes through a single leak. In future work, more complex leak configurations and the applicability of this method in real buildings have to be investigated. Microphone arrays could be used to detect leaks. As soon as the leak locations are identified, the method introduced in this work could be used to estimate leak sizes.

NOMENCLATURE

ΔP	=	Pressure difference	[Pa]
ρ	=	Density of air	[kg/m³]
A	=	Cross-sectional area of Venturi tube	[m²]
C	=	Flow coefficient	[m³/(h Pa^n)]
C_{xy}	=	Coherence function	[-]
G_{xy}	=	Cross-spectral density between time signal x and y	[W/Hz]
G_{xx}	=	Auto-spectral density between time signal x and x	[W/Hz]
G_{yy}	=	Auto-spectral density between time signal y and y	[W/Hz]

n	=	Pressure exponent	[-]
Q	=	Airflow rate	[m³/h]
x, y	=	Discrete time signals	[s]

REFERENCES

ASTM. 2017. ASTM E1186-17, *Standard Practices for Air Leakage Site Detection in Building Envelopes and Air Barrier Systems*. West Conshohocken, PA: ASTM International.

ASTM. 2019. ASTM E779-19, *Test Method for Determining Air Leakage Rate by Fan Pressurization.* West Conshohocken, PA: ASTM International.

CAN/CGSB. 2019. CAN/CGSB 149.10-2019, *Determination of the Airtightness of Building Envelopes by the Fan Depressurization Method*. Gatineau: Canadian General Standards Board.

Chelliah, Kanthasamy, Ganesh Raman, and Ralph T. Muehleisen. 2017. An Experimental Comparison of Various Methods of Nearfield Acoustic Holography. *Journal of Sound and Vibration* 403:21–37.

Benesty, Jacob and Yiteng Huang. 2013. *Adaptive Signal Processing: Applications to Real-World Problems.* Heidelberg: Springer Berlin Heidelberg

DIN. 2018. *DIN EN ISO* 9972:2018-12, *Thermal Performance of Buildings - Determination of Air Permeability of Buildings - Fan Pressurization Method.* Berlin: Beuth Verlag GmbH.

International Energy Agency. 2011. *Energy-Efficient Buildings: Heating and Cooling Equipment. IEA Technology Roadmaps.* Paris: OECD Publishing.

Muehleisen, Ralph T., and Kanthasamy Chelliah. 2018. SonicLQ: An Acoustic Method for Locating and Sizing Air Leaks in Building Envelopes. *INTER-NOISE and NOISE-CON Congress and Conference Proceedings* 258:663–69

Ng, Lisa C., Amy Musser, Andrew K. Persily, and Steven J. Emmerich. 2013. Multizone Airflow Models for Calculating Infiltration Rates in Commercial Reference Buildings. *Energy and Buildings* 58:11–18.

Reader-Harris, Michael. 2015, *Orifice Plates and Venturi Tubes.* Cham: Springer International Publishing.

Shannon, Claude Elwood. 1949. Communication in the Presence of Noise. *Proceedings of the IRE* 37(1):10–21.

Varshney, Kapil, Javier E. Rosa, Ian Shapiro, and Daniel Scott. 2013. Air-Infiltration Measurements in Buildings Using Sound Transmission Loss Through Small Apertures. *International journal of green energy* 10(5):482–93.

Vornanen-Winqvist, Camilla, Kati Järvi, Sander Toomla, Kaiser Ahmed, Maria A. Andersson, Raimo Mikkola, Tamás Marik, László Kredics, Heidi Salonen, and Jarek Kurnitski. 2018. Ventilation Positive Pressure Intervention Effect on Indoor Air Quality in a School Building with Moisture Problems. *International journal of environmental research and public health* 15(2).

Walker, I. S., and D. J. Wilson. 1998. Field Validation of Algebraic Equations for Stack and Wind Driven Air Infiltration Calculations. *HVAC&R Research* 4(2):119–39.